Combining circulating tumor cell and circulating cell free DNA analyses enhances liquid biopsy sensitivity in detecting high grade serous tubo-ovarian carcinoma

Beatrice Cavina[1,2], Simona Corrà[1,2], Camelia Alexandra Coadă[1,2], Monica De Luise[1,2], Silvia Lemma[1,2], Sara Coluccelli[3], Antonio De Leo[1,3], Stella Di Costanzo[4], Francesco Mezzapesa[4], Giulia Girolimetti[1,2], Pierandrea De Iaco[1,4], Anna Maria Porcelli[5,6], Anna Myriam Perrone[1,4], Dario de Biase[3,5], Giuseppe Gasparre[1,2,7], Ivana Kurelac[1,6,#]

[1]Department of Medical and Surgical Sciences (DIMEC), University of Bologna, Bologna, Italy.
[2] Centre for Applied Biomedical Research, University of Bologna, Bologna, Italy.
[3]Solid Tumor Molecular Pathology Laboratory, IRCCS Azienda Ospedaliero-Universitaria di Bologna, Bologna, Italy.
[4]Division of Gynecologic Oncology, IRCCS Azienda Ospedaliero-Universitaria di Bologna, Bologna, Italy.
[5]Department of Pharmacy and Biotechnology (FABIT), University of Bologna, Bologna, Italy.
[6]IRCCS Azienda Ospedaliero-Universitaria di Bologna, Bologna, Italy.
[7]Centro Studi e Ricerca sulle Neoplasie Ginecologiche, University of Bologna, Bologna, Italy.

Corresponding author:
Ivana Kurelac, PhD
Department of Surgical and Medical Sciences, University of Bologna
IRCCS Azienda Ospedaliero-Universitaria di Bologna
Via Massarenti 9, 40138 Bologna, Italy
Phone: +39 051 2094735
Email: ivana.kurelac@unibo.it

Abstract

Background: Liquid biopsy is a promising strategy for detecting and monitoring neoplastic diseases, with circulating tumor cells (CTCs) and circulating tumor DNA (ctDNA) being the most common objects of investigation. Most analyses have focused on these biomarkers separately, and simultaneous detection has not yet been attempted in high grade serous tubo-ovarian carcinoma (HGSOC). The aim of our study was to assess whether the tandem CTC/ctDNA approach increases HGSOC detection efficiency of peripheral blood liquid biopsy.

Methods: For CTC detection, by using healthy donor samples spiked with known cancer cell numbers, we tested gene expression assays and *TP53* next-generation sequencing (NGS). The latter was also applied for ctDNA detection where analytical validity was ensured by calculating the optimal variant allele frequency (VAF) threshold for mutation calling. The clinical validity of the assays was then verified on two HGSOC cohorts and respective controls. Standard 2x2 contingency tables and Wilson method were used to evaluate clinical validity, by calculating specificity, sensitivity, and accuracy with 95% confidence intervals (CI).

Results: High analytical sensitivity and specificity were found for both gene expression and *TP53* NGS based CTC detection, as these assays specifically detected as few as five cancer cells spiked in control sample. Regarding clinical validity, the gene expression-based CTC detection showed 0.48 accuracy, 13.3% sensitivity, and 100% specificity, whereas *TP53* sequencing demonstrated better assay performance (0.77 accuracy, 46.7% sensitivity, 100% specificity). For circulating cell-free DNA (cfDNA) analysis, we first identified 0.31% VAF cut-off for accurate ctDNA *TP53* mutation calling. Subsequent clinical validity assessment showed solid performance efficiency of the ctDNA based liquid biopsy (0.71 accuracy, 60% sensitivity, and 100% specificity), outperforming the CTC detection methods.

Importantly, the tandem ctDNA/CTC analysis improved disease detection rate in both HGSOC cohorts, allowing to achieve, respectively, 73.3% and 93.3% sensitivity. Interestingly, *TP53* NGS

revealed CTC private variants, and shared ctDNA/CTC mutations undetected in the primary tissue, highlighting the ability of the dual-analyte approach to capture tumor heterogeneity and allow mutation cross-validation.

Conclusions: Our study reveals the complementary value of simultaneous CTC and cfDNA analysis in HGSOC, advancing the translational potential of liquid biopsy integration for the management of this disease.

Keywords

Liquid biopsy; High grade serous tubo-ovarian carcinoma; Circulating tumor cells; Circulating tumor DNA; *TP53* genotyping

List of abbreviations

American College of Medical Genetics and Genomics (ACMG)

Area Under the Curve (AUC)

Circulating cell-free DNA (cfDNA)

Circulating tumor cells (CTCs)

Circulating tumor DNA (ctDNA)

Confidence interval (CI)

Digital PCR (dPCR)

Epithelial cell adhesion molecule (EpCAM)

Formalin fixed paraffin embedded (FFPE)

Green fluorescent protein (GFP)

High grade serous tubo-ovarian carcinoma (HGSOC)

Leave-One-Out cross-validation (LOOCV)

Low grade serous ovarian cancer (LGSOC)

84 Magnetic-activated cell sorting (MACS)

85 Neoadjuvant chemotherapy (NACT)

86 Next-generation sequencing (NGS)

87 Ovarian cancer (OC)

88 Peripheral blood (PB)

89 Peripheral blood mononuclear cell (PBMC)

90 Quantitative Real Time-PCR (qRT-PCR)

91 Receiver Operating Characteristic (ROC)

92 Variant allele frequencies (VAF)

93
94

Background

Liquid biopsy, in terms of searching for tumor derived material in peripheral blood (PB) samples, has emerged as a revolutionary tool in oncology. It is a minimally invasive approach which allows easily repeatable sampling to monitor disease progression and holds great potential to be implemented for cancer screening [1]. Introducing efficient liquid biopsy in ovarian cancer (OC) setting would be particularly groundbreaking, especially in high grade serous tubo-ovarian carcinoma (HGSOC), the most common and most aggressive histotype, which in 80% of cases is diagnosed at advanced stages due to unspecific and late presentation of symptoms [2,3]. The HGSOC diagnosis relies on histological evaluation of invasive tumor biopsy and, currently, no existing general population screening protocol is available. Finding an appropriate method for recognizing the disease at earlier stages is the most cogent issue in the field, as catching HGSOC at stage I guarantees 91.7% 5-year survival rate, compared to 31.8% when it is diagnosed at stages III-IV [2]. Liquid biopsy approaches offer a promising solution for this challenge, as well as for improvement of patient follow-up in terms of relapse and therapy-response prediction, while reducing the use of invasive procedures. However, liquid biopsy workflows in HGSOC are still at an explorative phase.

Among others, circulating tumor cells (CTCs) and circulating tumor DNA (ctDNA) have been explored in the context of OC, mainly regarding progression monitoring. In particular, CTCs have been associated with worse overall and progression-free survival of OC patients [4,5], but lack of standardized methods for their detection has, so far, prevented such analysis from being implemented into everyday practice. Apart from the general difficulty in discriminating scant tumor-derived material in blood specimens, detection of CTCs in OC is additionally challenged by the high molecular heterogeneity of this disease [6]. For example, whereas positivity for epithelial cell adhesion molecule (EpCAM) is an efficient marker to pinpoint CTCs in breast or lung malignancies [7,8], in OC patients, EpCAM+ cells circulating in PB are not necessarily

120 tumor derived [8]. One of the strategies designed to circumvent the issue of heterogeneity
121 envisions molecular marker agnostic CTC enrichment, such as Parsortix, and subsequent
122 multiple gene expression analysis [9,10]. However, there is no consensus on which gene panel
123 secures the highest specificity and sensitivity, and the efficiency of different enrichment methods
124 is rarely evaluated in a single study [6,11].
125 Regarding circulating cell-free DNA (cfDNA) analysis, works on HGSOC exploited *TP53*
126 mutations as a distinctive marker of ctDNA [12–15], since this gene is mutated in nearly all cases
127 of HGOSC [16,17]. However, hotspot analysis is not feasible for tumor suppressors unless the
128 variant is known *a priori*, and untargeted next-generation sequencing (NGS) of cfDNA often
129 detects variant allele frequencies (VAF) <0.5, which are not considered to be highly specific
130 markers [14]. Indeed, there is no generally accepted VAF cut-off value for ctDNA *TP53* variant
131 calling specifically in the context of HGSOC.
132 Interestingly, oncologic liquid biopsy studies have up to date been mainly focusing on either
133 CTC or ctDNA detection separately, rarely performing multianalyte assessment in the same
134 blood sample, even though it is emerging that the two analytes are not redundant biomarkers, but
135 provide complementary information [18,19]. In this scenario, the clinical impact of tandem CTC
136 and ctDNA detection has never been explored in HGSOC and still lacks a formal evaluation.
137 To converge towards the development of efficient liquid biopsy test for HGSOC detection, the
138 aim of this study was to prove that including both analytes in the workflow increases sensitivity.
139 We set up nucleic acid-based assays for CTC and ctDNA identification and evaluated their
140 analytical and clinical validity, which are critical parameters in any liquid biopsy assay
141 development [1]. By applying these optimized assays on two HGSOC patient cohorts, we
142 demonstrate for the first time that, compared to single analyte approaches, the combination of
143 CTC and ctDNA analyses improves the disease detection rate.
144

145 **Methods**

146 **Aim, design and setting of the study**

147 The primary aim was to demonstrate that CTC analysis coupled to ctDNA assay increases liquid
148 biopsy-based disease detection rate in HGSOC patients compared to single analyte approach.
149 The secondary aim was to improve standardization of liquid biopsy for HGSOC. We first
150 developed specific assays for each analyte of interest, ensured the analytical validity and then
151 evaluated the clinical validity (Figure 1A). For CTC analysis, we compared two enrichment
152 methods (Parsortix and CD45 negative selection) and tested three nucleic acid-based detection
153 techniques: (i) gene expression assays based on cDNA preamplification coupled to quantitative
154 Real Time-PCR (qRT-PCR); (ii) gene expression detection via digital PCR (dPCR); and (iii) CTC
155 mutation identification by *TP53* NGS with Ion AmpliSeq HD laboratory-developed panel
156 (Thermo Fisher Scientific). Analytical validity of each CTC detection approach was evaluated
157 by using healthy donor PB spiked with known numbers of cancer cells, whereas clinical validity
158 was evaluated by analyzing HGSOC patients and healthy controls. For ctDNA detection, *TP53*
159 NGS with Ion AmpliSeq HD laboratory-developed panel (Thermo Fisher Scientific) was used.
160 Analytical validity was ensured by setting the VAF threshold which most accurately identifies
161 primary tumor mutations in plasma cfDNA, whereas clinical validity was evaluated by analyzing
162 HGSOC and low grade serous ovarian cancer (LGSOC) patients since the latter lack *TP53*
163 mutations. To demonstrate that including CTC analysis provides more informative liquid biopsy,
164 compared to ctDNA approach alone, two separate HGSOC cohorts (n=15 each) were enrolled in
165 which for each patient both CTC enriched fraction and plasma cfDNA were analyzed (Figure
166 1B-D). In cohort 1, CTC enriched fraction was analyzed by gene expression assay, whereas in
167 cohort 2, CTCs were evaluated via *TP53* NGS. The latter was also applied for cfDNA analysis
168 in all 30 patients. Finally, the disease detection rates obtained by CTC and ctDNA assays were
169 compared within each cohort.

Figure 1 Study design and overview of HGSOC patient characteristics. (A) *Flowchart reporting the analytical and clinical validity evaluation implemented for CTC and ctDNA detection assays on liquid biopsy samples.* ***(B)*** *Demographic and clinical data of HGSOC patients enrolled for the study, with colored squares describing the analyses for which the patient material was used.* ***(C-D)*** *Summaries of demographic and clinical data of cohort 1* ***(C)*** *and cohort 2* ***(D)*** *enrolled for the study. International federation of gynecology and obstetrics (FIGO) staging and clinical status are indicated.*

Patients and healthy controls enrolment

For validation of OC CTC gene expression markers, primary tumor tissues of four advanced stage (III, IV) and four early stage (I, II) HGSOC patients who underwent debulking surgery in period between May 2016 and October 2019 were analyzed, together with three PB mononuclear cell (PBMC) samples derived from healthy controls (Supplementary Table 1). Liquid biopsy samples were collected between September 2020 and March 2025, from HGSOC patients who

underwent surgery, either primary or interval debulking, at diagnosis or at the disease relapse (n=30, Figure 1B). Inclusion criteria comprised histologic diagnosis of HGSOC, presence of macroscopic disease at surgery in newly diagnosed and relapsed patients, as well as in subjects post neoadjuvant chemotherapy (NACT). Peripheral blood samples used as controls for determining the specificity of CTC analysis via gene expression (n=13), and for analytical validity assessment of CTC detection via *TP53* sequencing (n=4), derived from healthy female donors (inclusion criteria: women aged ≥ 25, with no history of oncologic disease; exclusion criteria: pregnancy, history of oncologic disease) (Supplementary Table 1). Controls for clinical validity assessment of ctDNA *TP53* deep sequencing were patients newly diagnosed with advanced stage LGSOC, whose liquid biopsy was collected between September 2019 and April 2023 (n=6, Supplementary Table 1). *Post-hoc* power calculations were performed using Clincalc [20]. Regarding CTC gene profiling, 88.4% *post hoc* power was calculated to estimate accuracy with alpha of 0.05, considering case *versus* control incidence of 52.5% and 0%, as previously published when using the same method [9]. Since *TP53* sequencing was never used for CTC detection of HGSOC up to date, we considered 66.7% case incidence reported in a breast cancer study which used a mutation-based liquid biopsy assay [21], and 83% *post hoc* power to estimate accuracy with alpha of 0.05 was calculated. Finally, for ctDNA detection, the subjects enrolled for clinical validation allowed 98.8% *post-hoc* statistical power to estimate efficiency, considering 0.05 alpha and case *versus* control incidence of 73% and 0%, respectively [22].

The study was conducted in accordance with the Declaration of Helsinki and the protocol was approved by the Independent Ethics Committee "Comitato Etico di Area Vasta Emilia Centro" (Protocol EM363-2024_107/2011/U/Tess/AOUBo). All subjects enrolled in the study provided written informed consent for their participation.

Cell lines

206 OV90 (#ATCC-CRL-3585) and SKOV3 (#ATCC-HTC-77) cells were purchased from ATCC,
207 whereas OC314 (RRID: CVCL_1616) cell line was kindly gifted by Prof. Ada Funaro
208 (University of Turin). Cells were authenticated using AMPFISTRIdentifiler kit (Applied
209 Biosystems #4322288), confirming their putative STR profile. Cells were regularly screened for
210 mycoplasma and were cultured in RPMI 1640 (Euroclone #ECB9006L) supplemented with 10%
211 FBS South America origin EU Approved (Euroclone #ECS5000L), 2 mM L-glutamine
212 (Euroclone #ECB3000D), and 1% penicillin/streptomycin (Euroclone #ECB3001D) in an
213 incubator at 37°C with a humidified atmosphere at 5% CO2. EVOS M5000 Imaging System
214 (ThermoFisher Scientific #AMF5000) was used for cell line monitoring.

215 **Lentiviral transduction of green fluorescent protein (GFP) in SKOV3 cells**

216 Lentiviral particles expressing GFP were produced using HEK293T cells, seeded in 10 cm tissue
217 culture dishes at 40-50% confluency and incubated overnight. At 80% confluence, cells were
218 transfected using Xtreme Gene Roche Transfection reagent (Cat. No. 6366236001, Roche)
219 according to manufacturer's instructions. Specifically, the transfection mixture consisted of 7.5
220 µg psPAX2 packaging plasmid and 2.5 µg pMD2-VSVG envelope plasmid, 10 µg GFP-
221 expressing lentiviral plasmid, (total DNA: 20 µg), diluted in 2 mL Opti-MEM medium.
222 Packaging and envelope plasmids were a kind gift from Prof. Marco Montagner (University of
223 Padova), whereas the GFP-expressing plasmid was a kind gift from Dr. Ilaria Malanchi [23].
224 Xtreme Gene transfection reagent was added to the DNA with a ratio of 1:3, incubated for 15
225 min at room temperature, and then added dropwise to the HEK293T cells. Concomitantly,
226 SKOV3 recipient cells were seeded in a T25 flask at 20-30% confluency to achieve optimal cell
227 density for transduction the following day. Viral supernatant was harvested 48 hours post
228 HEK293T transfection and filtered through 0.45 µm syringe filters to remove cellular debris. For
229 SKOV3 transduction, filtered viral particles were mixed 1:1 with fresh culture medium
230 supplemented with polybrene (final concentration: 8 µg/mL) to enhance viral uptake efficiency.

231 SKOV3 cells were incubated with the virus-containing medium for 48 hours. Clonal selection
232 was performed to identify the cells with the highest GFP expression, which was checked with
233 EVOS M5000 Imaging System (Thermo Fisher Scientific #AMF5000), and a pool of 30 clones
234 was made for use in the subsequent experiments.

235 **Spiked samples preparation**

236 Healthy donor PB (7.5 mL) was collected in 10 mL EDTA tube and manually spiked within 24
237 hours with known numbers of SKOV3^{GFP} cells: 0, 5, 50, 500, 5'000, or 500'000. In detail,
238 SKOV3 were trypsinized (Sigma #T4049) and counted using Neubauer chamber with Trypan
239 Blue (Sigma #T8154) staining to exclude dead cells. A PBS suspension (200 µL) of 500, 5'000
240 or 500'000 live cells was then added to PB. To prepare PB samples carrying five, and 50
241 SKOV3^{GFP} single-cell picking was performed: trypsinized cells were diluted in PBS solution,
242 visualized with phase-contrast microscopy under the sterilized hood, individually picked using
243 10 µL pipette tip and collected in 1.5 mL Eppendorf tube. PBS was eventually added to final
244 volume of 200 µL and spiked in PB. The same amount of PBS alone was used as a negative
245 control (0 SKOV3^{GFP}). Spiked samples were then enriched using Parsortix or CD45 negative
246 sorting for downstream analysis. EVOS M5000 Imaging System (Thermo Fisher Scientific
247 #AMF5000) was used to confirm the presence of SKOV3^{GFP} prior to elution.

248 **CTC enrichment**

249 At least 7.5 mL of PB was processed for microfluidic-based CTC enrichment by using Parsortix®
250 Cell Separation System (ANGLE) with GEN3D6.5 Cell Separation cassettes according to the
251 manufacturer's instructions. Default pressure protocol was used, and the captured cells were
252 eluted in 1.2 mL of PBS. For negative affinity-based CTC enrichment, PB was processed using
253 automatic magnetic-activated cell sorting (MACS) for CD45 negative selection. Red Blood Cell
254 Lysis Solution (Miltenyi Bioitec #130-094-183) was used to lyse erythrocytes, and human CD45
255 MicroBeads (Miltenyi Bioitec #130-045-801) were employed to deplete CD45+ leukocytes,

256 following the manufacturer's protocol. The stained cell suspension was sorted using
257 AutoMACS® (Miltenyi Biotec) with protocol Depl05 [24]. CTC-enriched solutions obtained
258 from both Parsortix and AutoMACS were centrifuged at 1'200 rpm for 5 min and the pellets
259 were resuspended in 350 µL of RLT buffer for subsequent RNA extraction. For DNA extraction,
260 Parsortix CTC enriched fraction was centrifuged at 1'200 rpm for 5 min and the pellet was stored
261 at -80°C for the subsequent analysis.

262 **Nucleic acid extraction**

263 RNA extraction from tumor biopsies, cell lines, and CTC-enriched fractions was performed using
264 RNeasy Mini Kit (QIAGEN #74106), while for DNA isolation from formalin fixed paraffin
265 embedded (FFPE) samples Maxwell® CSC DNA FFPE Kit (Promega, #AS1350) was used.
266 Nucleic acid concentrations were assessed with NanoDrop (Thermo Fisher) and stored at -20°C.
267 Peripheral blood for cfDNA analysis was processed within 2 hours from withdrawal and we
268 performed a two-step plasma preparation protocol. In detail, the 10 mL EDTA tube was
269 centrifuged at 3'500 g for 15 min at 4°C, and then plasma was further centrifuged for 10 min at
270 maximum speed. Plasma was stored at -80°C until cfDNA extraction, as we previously confirmed
271 that our preanalytical handling does not affect the downstream analysis. *Quick*-cfDNA
272 Serum&Plasma Kit (Zymo research #D4076) was used for plasma cfDNA extraction, eluted in a
273 final volume of 30 µL. DNA was isolated from CTC enriched fractions by using QIAamp DNA
274 Blood mini kit (QIAGEN #51106) and eluted in a final volume of 30 µL. The same kit was used
275 also for DNA extraction from patients derived PBMC. cfDNA and CTC derived DNA were
276 quantified using Qubit™ (Invitrogen) with High Sensitivity dsDNA assay kit (Invitrogen
277 #Q32851) and stored at -20°C. Liquid biopsy DNA concentration was calculated based on ng/µL
278 eluted after extraction from plasma or CTC-fraction, quantified fluorometrically by using Qubit
279 HS assay, multiplied by µL used and finally divided by either the total mL of plasma analyzed or
280 the total mL of enriched PB.

281 **cDNA synthesis and preamplification**

282 High-Capacity cDNA Reverse Transcription Kit (Applied Biosystem #4368814) was used for
283 cDNA preparation with random hexamers starting from different RNA concentrations based on
284 samples. When available, 100 ng of RNA was used for cDNA synthesis and we used the
285 maximum possible RNA quantity (14 µL) for CTC-enriched samples, independently from their
286 starting concentration. Reaction was performed using T100 Thermal Cycler (Bio-Rad) following
287 the protocols: 25°C 10 min, 37°C 120 min, 85°C 5 min. A total of 20 µL concentrated cDNA was
288 obtained. For the following preamplification reaction cDNA diluted 1:2 was used as starting
289 material, added with TaqMan® PreAmp Master Mix (2X) (Thermo Fisher Scientific #4384267)
290 and TaqMan gene expression assay of interest pooled at a final concentration of 0.2X, according
291 to the manufacturer's instructions. Reaction was performed using T100 Thermal Cycler (Bio-
292 Rad) following the protocols: 95°C 10 min; 95°C 15 sec and 60°C 4 min, for 14 cycles, 99°C 10
293 min. For the downstream gene expression analysis, native cDNA was diluted 1:5, while PA cDNA
294 was diluted 1:2.

295 **Gene expression quantitative real-time PCR (SybrGreen and TaqMan)**

296 Quantitative RT–PCR was performed using either the intercalating dye SYBR Green dye
297 (Promega) or 5' nuclease probes PrimeTime™ qPCR Probes (TaqMan assay). For the SYBR
298 Green assay, the primer sequences were designed using Primer3 software [25], the presence of
299 3' intra/inter primer homology was excluded using the IDT OligoAnalyzer tool [26] and the
300 availability of the target sequence was estimated by predicting cDNA secondary structure by the
301 Mfold web server [27]. Forward and reverse primers sequences for each target are listed in
302 Supplementary Table 2. For TaqMan assays, the qPCR Probes assay for each gene was selected
303 on the Thermo Fisher website [28], and the predesigned qPCR assays recommended by the
304 manufacturer were used. qRT–PCR with SYBR Green assay was performed with GoTaq qPCR
305 Master Mix (Promega #A6002) and run in 7500 Fast Real-Time PCR System (Applied

306 Biosystem), using the following conditions: 95°C 5 min; 45 cycles of 95°C 15 sec and 63°C 45
307 sec. The qRT–PCR with TaqMan assay was performed with GoTaq R Probe qPCR Master Mix
308 (Promega #A6101 and #A6102) and run in the abovementioned system, using the following
309 conditions: 95°C 2 min; 40 cycles of 95°C 15 sec and 60°C 1 min.

310 **Digital PCR**

311 Digital PCR assay was performed using Absolute Q™ DNA Digital PCR Master Mix (5X)
312 (Thermo Fisher Scientific #A52490), TaqMan assay selected for gene expression analysis, and
313 10 ng of cDNA according to manufacturer's instructions. The MAP16 plate kit (Thermo Fisher
314 Scientific #A52865) was loaded and run on Absolute Q 22120661 instrument, using the
315 following conditions: 50°C 2 min, 96°C 10 min; 40 cycles of 96°C 5 sec and 60°C 15 sec. The
316 downstream analysis was performed using QuantStudio Absolute Q Software Version 6.3.

317 **Sequencing of *TP53***

318 To comprehensively characterize *TP53* genotypes across different sample types, we employed
319 distinct sequencing approaches as follows. Primary tumor tissue was macro dissected from FFPE
320 blocks, DNA was extracted and sequenced using the previously validated NGS laboratory-
321 developed multi-gene panel [29], covering 21.77 kb with 330 amplicons, including *TP53* CDS,
322 as already described in [30]. Mutations were considered valid if present in at least 5% of the total
323 number of analyzed reads and observed in both strands, as *per* previously established validation
324 criteria [31]. The somatic nature of the identified primary tumor mutations was confirmed by
325 Sanger sequencing of matched PBMC following the standard protocol [30]. Liquid biopsy-
326 derived samples (i.e., cfDNA and CTC enriched fraction-derived DNA) were sequenced using
327 the Ion AmpliSeq HD laboratory-developed panel (Thermo Fisher Scientific) targeting the entire
328 coding sequence (CDS) of *TP53* (NM_000546.6, human reference genome hg19/GRCh37),
329 overall covering 1.71 Kb with 39 amplicons. Single-nucleotide variants/Indels present in at least
330 0.2% of the total number of analyzed reads were considered for variant calling [32–34]. The

331 latter liquid biopsy panel with 0.2% VAF cut-off was also used for sequencing healthy donor
332 control-derived PBMC during analytical validity evaluation for CTC detection, as well as for
333 HGSOC patient-derived PBMC samples sequenced to exclude clonal hematopoiesis as the
334 source of variants found in liquid biopsies. For NGS library preparation, approximately 10 ng of
335 liquid biopsy-derived DNA or 30 ng for FFPE-derived DNA were processed. Sequencing was
336 carried out on an Ion 530 chip. The data were analyzed with the Ion Reporter tool (version 5.20,
337 Thermo Fisher Scientific) and IGV software [35,36] (Integrative Genome Viewer version
338 2.12.2). Variant classification was performed using American College of Medical Genetics and
339 genomics (ACMG) guidelines with the Varsome database [37,38].

340 **Statistical analyses**

341 The statistical analyses were performed using R version 4.3.1 with the *pROC*, *dplyr*, *ggplot2*,
342 *binom*, and *presize* packages. Clinical validity was assessed using standard 2x2 contingency
343 tables, which allow calculation of specificity, sensitivity, accuracy, positive predictive value, and
344 negative predictive value. Accuracy estimates of clinical sensitivity and specificity were
345 determined with exact 95% confidence intervals (CI) using the Wilson method. Fisher's exact
346 test assessed associations between patient group and test results. The Mann-Whitney U test was
347 applied to compare cfDNA VAF between tumor biopsy-specific vs liquid biopsy only variants.
348 For VAF threshold optimization, Receiver Operating Characteristic (ROC) curve analysis was
349 performed to identify the best ctDNA VAF threshold via Youden's J statistic. The same data set
350 was used for running Leave-One-Out cross-validation (LOOCV) to account for model
351 generalizability, which provided the threshold and relative Area Under the Curve (AUC) for each
352 iteration. ROC statistical significance was evaluated using permutation testing and the Hanley-
353 McNeil Z-test against the null hypothesis of AUC=0.5. Age and cfDNA concentration differences
354 between HGSOC and LGSOC patients were compared using Student's t-test (GraphPad Prism

355 8). Statistical significance was defined as $p < 0.05$. Data visualization was performed using
356 GraphPad Prism 8, R version 4.3.1, and BioRender.com.
357
358 **Results**
359 **The optimized three-gene expression assay displays high analytical specificity and**
360 **sensitivity in detecting low cancer cell numbers in simulated liquid biopsies**
361 High inter-patient heterogeneity and ambiguous EpCAM expression in CTCs and PB cells have
362 thus far hampered identification of specific molecular targets for OC CTC detection [39–41].
363 Previous studies have tried to overcome the issue by relying on techniques which allow multiple
364 marker analysis [6,42,43], the most common strategy being gene expression detection via
365 multiplex qRT-PCR [4,9,10,43,44]. Since there is no consensus on which combination of genes
366 provides the best specificity and sensitivity of such an approach, we first focused on the design
367 and evaluation of an HGSOC gene panel to specifically recognize CTC. The literature search for
368 studies reporting OC CTC gene expression generated a list of 21 targets (Supplementary Table
369 3), which we validated in a subset of primary tumor tissues deriving from high and low stage
370 HGSOC patients, as well as in PB of three healthy controls (Supplementary Table 1) to account
371 for panel specificity. Most genes (76.2%) were expressed in all tumors, and only *AGR2* resulted
372 to be a less sensitive OC marker, with its expression being observed specifically in high stage
373 HGSOC (Figure 2A). However, nine out of 21 tested genes were also expressed in control
374 samples. This prompted us to test the specificity of the remaining 12 genes in an additional cohort
375 of healthy donor controls (n=10, Supplementary Table 1), by applying TaqMan probe chemistry
376 and cDNA preamplification to increase sensitivity. The results revealed low specificity of
377 *EPCAM*, *ERBB2*, *ERBB3*, *MAL2* and *MUC1*, as these genes were found expressed in 50-80%
378 native cDNA and in 80% of pre-amplified healthy controls (Figure 2B). The analysis of pre-
379 amplified cDNA revealed low specificity also for *PGR, LAMB1, PRAME* and *CDH3*, as they

380 were detected in 30-50% of control samples. On the other hand, *AGR2*, *GPX8* and *WT1* were not
381 expressed in the healthy control cohort and were thus defined as specific HGSOC CTC markers
382 in the context of liquid biopsy (Figure 2B-C).
383 Next, we sought to determine which workflow ensures analytical validity for CTC detection via
384 three-gene assay. We used simulated liquid biopsy samples in which known numbers of cancer
385 cells were spiked into healthy donor PB. To choose the optimal model for simulated liquid biopsy
386 preparation, *AGR2*, *GPX8* and *WT1* expression was evaluated in a set of HGSOC cell lines. The
387 highest expression was found in SKOV3 cells (Supplementary Figure 1A), which were then
388 labelled with Green Fluorescent Protein (GFP) to track them during isolation protocols
389 (Supplementary Figure 1B). To mimic the rare cancer cells found in patient liquid biopsies, PB
390 was spiked with five or 50 SKOV3 cells, whereas unspiked samples and spiking 500,000 cells
391 represented negative and positive controls, respectively (Figure 2D). With the secondary aim of
392 comparing CTC enrichment methods, we processed the samples with the two most widely used
393 cancer marker agnostic enrichment approaches, namely Parsortix and CD45 negative magnet
394 assisted cell sorting. The results showed that if samples carrying low cell numbers were not
395 enriched before gene expression analysis, no amplification signals were detected, regardless of
396 the preamplification step (Figure 2E, grey graph). On the other hand, both enrichment protocols
397 allowed detection of even five cancer cells if the cDNA was pre-amplified (Figure 2E, orange
398 graphs), revealing comparable cancer cell recovery efficiency between Parsortix and CD45-
399 negative sorting. Of note, all three genes were detected in samples spiked with 50 cancer cells,
400 whereas only *GPX8* was found in samples carrying five SKOV3 cells (Supplementary Figure
401 1C). We furthermore investigated whether gene expression analysis via dPCR could provide
402 similar or better sensitivity while avoiding the preamplification step, however such an approach
403 was unable to identify samples spiked with five cells and generally showed lower sensitivity for
404 each of the three genes analyzed (Figure 2F, Supplementary Figure 1D-E).

Taken together, it may be concluded that the three-gene panel analysis, coupled with agnostic enrichment and cDNA preamplification step, is sufficiently sensitive for detection of very low cancer cell numbers, hence tackling the main challenge of CTC-based liquid biopsies.

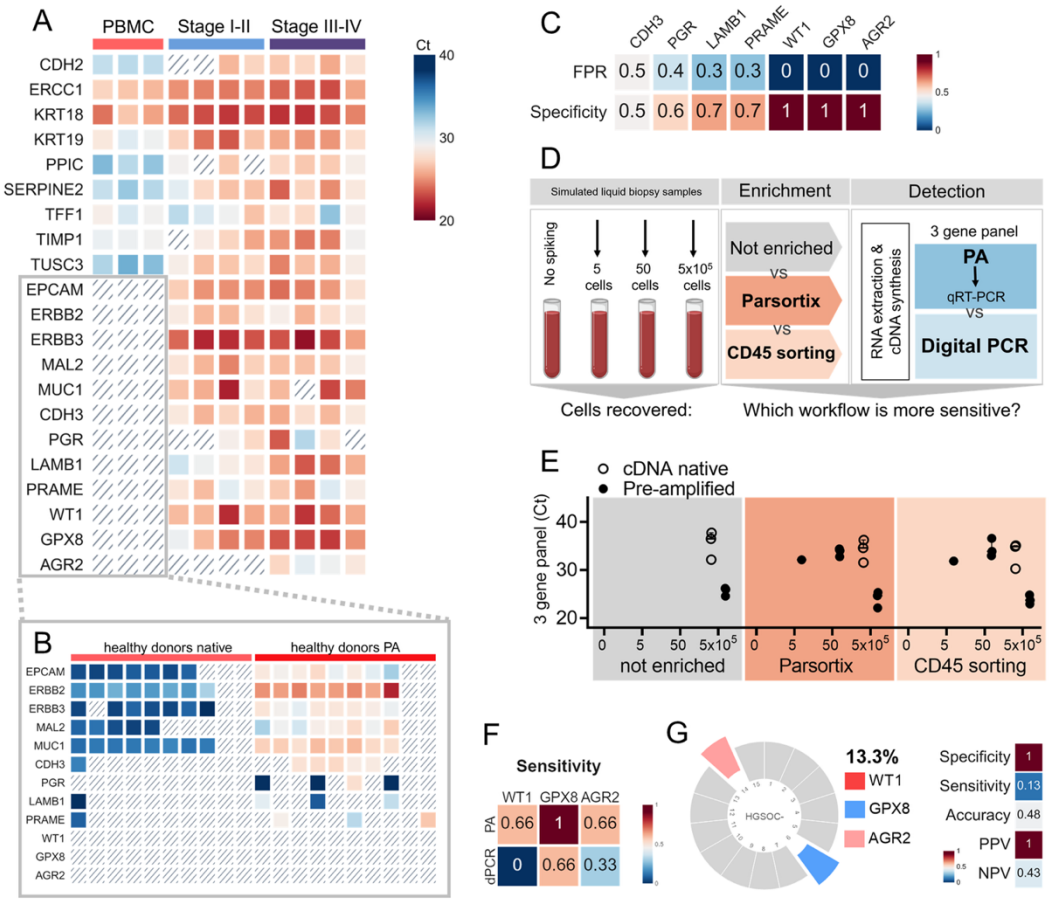

Figure 2. Analytical and clinical validity assessment of the gene expression-based CTC detection in HGSOC patients. (A) *Cycle-threshold (Ct) heatmaps obtained via qRT-PCR of RNA extracted from three healthy donor PBMCs, eight primary tumors derived from HGSOC patients. Slashed boxes indicate undetected transcripts.* ***(B)*** *Cycle-threshold (Ct) heatmaps obtained via qRT-PCR of RNA extracted from PBMCs of ten healthy donors with native or preamplifed (PA) cDNA. Slashed boxes indicate undetected transcripts.* ***(C)*** *Heatmap reporting false positive rate (FPR) and specificity values calculated for each gene.* ***(D)*** *Graphical sketch of the experimental workflow designed to compare enrichment and detection methods by using simulated liquid biopsy samples.* ***(E)*** *Dot plot reporting Cycle-thresholds (Ct) obtained via qRT-PCR of RNA extracted from healthy donor PB spiked with 0, 5, 50, or 500'000 SKOV3 cells. Gray-graph shows not enriched samples. Dark and light orange-graphs show samples enriched with Parsortix and CD45 negative selection, respectively. Native and PA cDNA transcripts are indicated with empty and full circles, respectively.* ***(F)*** *Heatmap reporting sensitivity values calculated for each gene by PA cDNA qRT-PCR (PA) and dPCR detection methods.* ***(G)*** *Pie chart indicating the disease detection rate of liquid biopsy analysis via Parsortix enrichment coupled with WT1/GPX8/AGR2 CTC detection, and the heatmap reporting the corresponding performance metrics. PPV-positive predictive value; NPV-negative predictive value*

Gene expression profiling identifies CTC specific transcripts in a subset of HGSOC liquid biopsies

Once analytical validity was ascertained, we sought to assess the clinical validity of the three-gene panel analysis to detect HGSOC in the CTC-enriched fraction. Regarding the enrichment

426 method, Parsortix was selected as a more suitable procedure due to its marker agnostic property,
427 lower operator hands-on time, and because it potentially captures CTC clusters, otherwise
428 discarded with CD45 negative sorting [11,45,46]. A cohort of 15 HGSOC cases (cohort 1) was
429 enrolled in the study (Figure 1) and liquid biopsies were processed with Parsortix enrichment
430 coupled with the *AGR2*-*GPX8*-*WT1* detection. Only two positive cases were identified, resulting
431 in 0.48 accuracy, 13.3% sensitivity (95% CI: 3.7-37.9 %) and 100% specificity (95% CI: 72.2-
432 100 %) in detecting HGSOC via CTC gene profiling (Fisher's exact test p=0.5) (Figure 2G).
433 Concordantly with the high heterogeneity of HGSOC, different genes of the panel (*AGR2* and
434 *GPX8*) were found expressed in the two positive patients, HGSOC-6 and HGSOC-14,
435 respectively, suggesting the necessity of a multi-marker approach in increasing performance.
436 Considering the cohort was composed of advanced disease cases, with high macroscopic burden
437 at surgery and high probability of hematogenous spread, it may be concluded that here applied
438 three-gene expression panel is able to detect HGSOC in a low number of patients.

439 **Optimization of mutation calling ensures analytical validity of *TP53* next-generation**
440 **sequencing for ctDNA detection in HGSOC liquid biopsy**

441 The clinical value of ctDNA detection in liquid biopsy is being extensively investigated in
442 various cancers, including HGSOC where it is most often performed via sequencing of *TP53*
443 tumor suppressor, which is mutated in virtually all cases [16]. Most often, these analyses have
444 been performed via tumor-informed assays [12–14]. Rare studies dealing with tumor-agnostic
445 cfDNA *TP53* genotyping show promise [15] but call for caution regarding false positive results
446 [47], not infrequent when dealing with low VAF *TP53* variants in plasma cfDNA due to clonal
447 hematopoiesis [48]. Thus, we implemented high-depth *TP53* coding region sequencing of
448 cfDNA via Ion AmpliSeq™ HD high-sensitivity approach, to develop a tumor agnostic assay in
449 which PB ctDNA detection does not rely on previous knowledge about the primary tumor biopsy.

450 To avoid false positive calls, the first step in the analytical validity assessment was setting the
451 VAF threshold for the mutational call, which guarantees reliable ctDNA detection in liquid
452 biopsy (Figure 3A). Plasma, primary tumor tissue, and PBMC of 20 HGSOC patients were
453 collected and sequenced (Figure 1). We identified *TP53* variants in plasma cfDNA of 17 patients.
454 In total, 31 variants were found, 15 of which (48.39%) matched the primary tumor
455 (Supplementary Figure 2A), presenting median VAF of 1.38% (ranging from 0.2 to 26), and were
456 confirmed to be somatic events upon sequencing corresponding PBMC (Supplementary Figure
457 2B). Interestingly, the median VAF of the remaining 16 variants was significantly lower (0.27%,
458 ranging from 0.2 to 15.98), suggesting that mutations detected at higher frequencies are more
459 likely to be retrieved in the primary tumor biopsy (Wilcoxon-Mann-Whitney U Test p
460 value=0.006, Figure 3B). To define the most accurate VAF threshold that may discriminate
461 primary tumor driving events from rumor, we performed ROC analysis where solid biopsy
462 confirmed mutations were regarded as true positives and variants absent from matched primary
463 tumor as true negatives. The calculation of Youden's J factor across different VAFs identified
464 0.31% as the optimal cut-off, with AUC of 0.77 (SE±0.02, 95% CI 0.58-0.95, Permutation Test
465 p=0.01, Hanley-McNeil Z-test p=0.002) (Figure 3C). Given the limited sample size, we also
466 implemented LOOCV analysis to prevent overfitting. The test confirmed 0.31% as optimal cut-
467 off in 14 out of 17 iterations (82.35%, mean VAF 0.33%±0.05 SD) and revealed AUC values
468 ranging from 0.75 to 0.83 (mean training AUC 0.77; Figure 3D), demonstrating consistent
469 discriminative ability of the model.
470 Taken together, our optimization of the mutation calling provides evidence for analytical validity
471 of high-depth *TP53* sequencing for ctDNA detection in HGSOC liquid biopsies.

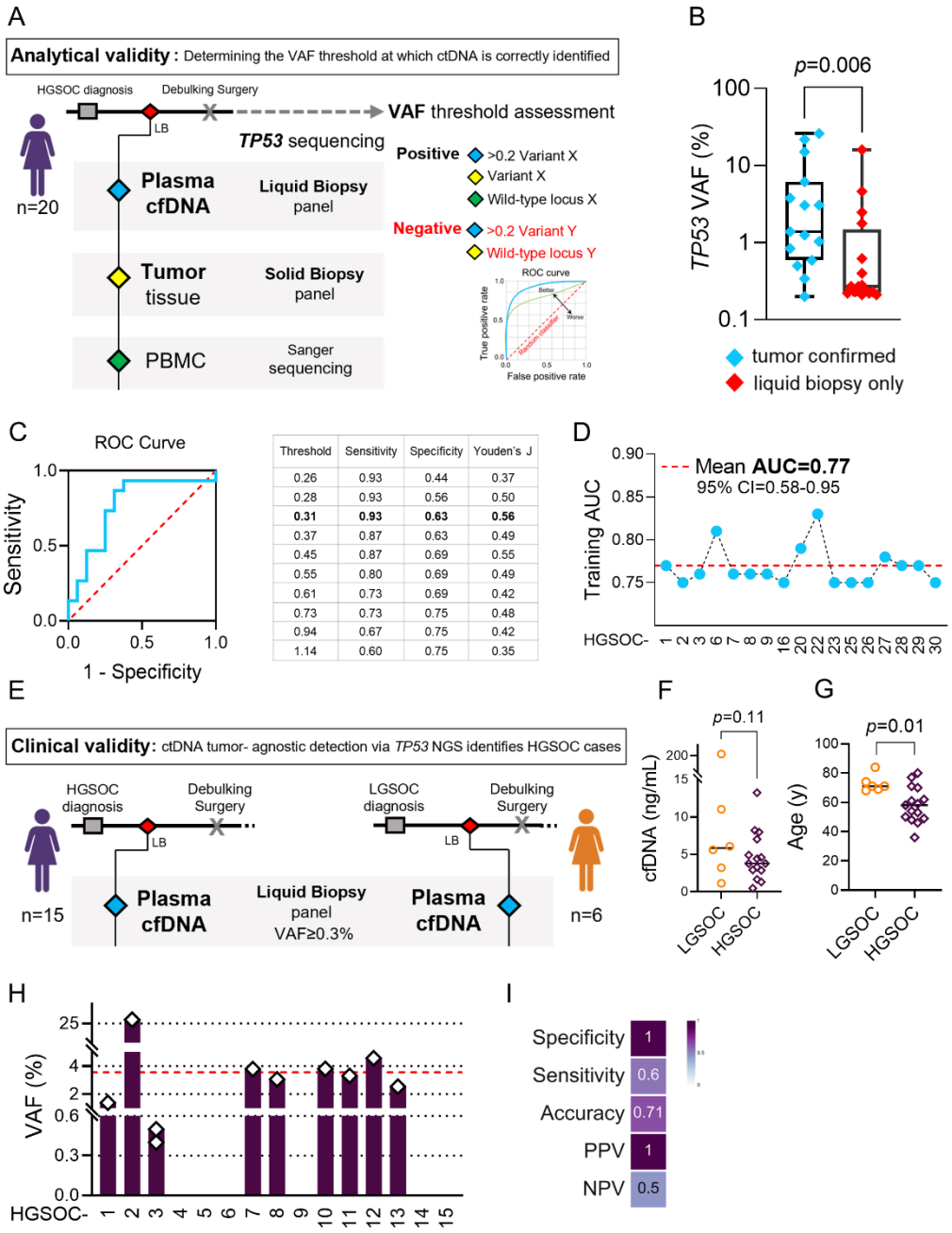

Threshold	Sensitivity	Specificity	Youden's J
0.26	0.93	0.44	0.37
0.28	0.93	0.56	0.50
0.31	**0.93**	**0.63**	**0.56**
0.37	0.87	0.63	0.49
0.45	0.87	0.69	0.55
0.55	0.80	0.69	0.49
0.61	0.73	0.69	0.42
0.73	0.73	0.75	0.48
0.94	0.67	0.75	0.42
1.14	0.60	0.75	0.35

Figure 3. Analytical and clinical validity assessment of tumor-agnostic TP53 NGS-based ctDNA detection in HGSOC. (A) *Graphical sketch of the workflow for definition of ctDNA detection VAF cut-off, performed by sequencing cfDNA variants in matched primary tumor tissue and PBMC.* ***(B)*** *Primary tumor confirmed (blue) and cfDNA private (red) TP53 VAFs found in HGSOC patients' plasma. P value indicates Mann-Whitney U test result.* ***(C)*** *ROC curve (blue) computed by considering tumor confirmed and cfDNA private TP53 VAFs as positive and negative category, respectively. Dashed red line indicates the random classifier. Adjacent table lists the sensitivity, specificity, and Youden's J calculated for each VAF threshold. The optimal cut-off value is indicated in bold.* ***(D)*** *Dot-plot reporting the LOOCV analysis training AUC results. The X axis reports HGSOC patient used to test the VAF threshold obtained from each iteration. Red dashed line indicates the mean AUC.* ***(E)*** *Graphical sketch of the workflow for clinical validity assessment. HGSOC and LGSOC liquid biopsies (LB) were used as positive and negative controls, respectively.* ***(F)*** *Median plasma cfDNA concentration in LGSOC (orange) and HGSOC (purple) patients. Single dots represent patients, black bars the computed median values, and p value indicates the t-test result.* ***(G)*** *Age in years (y) at liquid biopsy sampling of LGSOC (orange) and HGSOC (purple) patients. Single dots represent patients, black bars the computed median values, and p value indicates the t-test result.* ***(H)*** *TP53 VAFs found in plasma cfDNA of HGSOC cohort 1. Dashed red line indicates the median value.* ***(I)*** *Performance metrics heatmap of the tumor-agnostic TP53 ctDNA detection assay. PPV-positive predictive value; NPV-negative predictive value.*

488 **Customized *TP53* deep sequencing is a reliable approach for liquid biopsy-based detection**
489 **of HGSOC**

490 With the aim of measuring the performance of the test to reliably and reproducibly detect
491 HGSOC, the clinical validity was next assessed for the *TP53* NGS-based ctDNA assay (Figure
492 3E). Fifteen HGSOC patients from cohort 1 were considered as positive cases. As negative
493 controls, liquid biopsies derived from six LGSOC patients were collected (Supplementary Table
494 1), since they mimic tumor burden and corresponding high cfDNA concentration but lack *TP53*
495 mutations [49]. The LGSOC cohort showed comparable cfDNA concentrations (Figure 3F) but
496 was significantly older than the high-grade counterpart (Figure 3G). Since potential false
497 positives due to clonal hematopoiesis are expected to occur more likely in elderly subjects, the
498 age difference was not expected to bias the clinical validity assessment.

499

500 ***Table 1. TP53 variants and their allele frequencies found by cfDNA***
501 ***sequencing in liquid biopsies of cohort 1****. del=deletion; fs=frameshift*

HGSOC-	ctDNA VAF (%)	*TP53* variant
1	1.38	c.376-2A>G
2	26	p.T253_I254del
3	0.5	p.Q167Hfs*3
	0.4	p.Y205C
4	0	/
5	0	/
6	0	/
7	3.78	p.G245D
8	3.05	p.L201Ffs*8
9	0	/
10	3.8	p.E287Rfs*58
11	3.31	p.I195T
12	4.56	p.M246T
13	2.53	p.Y126*
14	0	/
15	0	/

502 Collectively, considering the defined 0.31% VAF threshold, all LGSOC derived cfDNA were
503 *TP53* wild-type, indicating 100% specificity of the assay. On the other hand, in the HGSOC
504 cohort, 10 *TP53* variants were identified in nine patients, with a median VAF of 3.55%, ranging
505 from 0.4% to 26% (Table 1, Figure 3H), revealing 0.71 accuracy, 60% sensitivity (95% CI: 37.5-
506 80.2%) and 100% specificity (95% CI: 61-100%) in detecting HGSOC via ctDNA approach
507 (Fisher's exact test p=0.01) (Figure 3I).
508 Taken together, our results establish clinical validity of cfDNA *TP53* sequencing as a sensitive
509 and specific approach for HGSOC detection via liquid biopsy and suggest 0.31% VAF threshold
510 for ctDNA mutation calling when the Ion AmpliSeq™ HD system is used.

511 **Simultaneous application of CTC and ctDNA identification assays improves HGSOC**
512 **detection via liquid biopsy**

513 The combined detection of CTC and ctDNA has demonstrated additional clinical value over
514 single-analyte approaches in various cancer types [21,50–52]. However, this dual strategy has
515 not yet been explored in the context of HGSOC, where it may offer substantial benefits to
516 patients if shown to improve the rate of disease detection. Therefore, we compared the data
517 obtained by the two assays in cohort 1 (Figure 4A), in which the presence of CTCs was evaluated
518 by gene expression. Four cases displayed concordant negativity (26.7%), whereas no cases
519 resulted positive for both assays. Interestingly, the two patients positive for CTCs were
520 concomitantly negative for ctDNA (13.3%), and nine patients positive for ctDNA were negative
521 for CTCs (60%), showing that the combinatory approach indeed increased HGSOC detection
522 rate compared to either single analyte assay (Figure 4B). Collectively, these results suggest that
523 including CTC identification in the workflow increases the disease detection rate from 60%,
524 obtained by the cfDNA-based analysis, to 73.3%, showing potential for improving the clinical
525 utility of liquid biopsy for HGSOC.

526 Driven by these results, we next sought to corroborate the finding in a second HGSOC cohort
527 and by applying a different CTC detection method. To harmonize the workflow and reduce
528 turnaround times of tandem CTC/ctDNA analysis, *TP53* liquid biopsy panel was chosen to detect
529 both analytes. To determine whether the approach provides high sensitivity and specificity for
530 CTC detection, analytical validity assessment was performed via *TP53* sequencing of the
531 Parsortix-enriched simulated liquid biopsies, prepared by spiking 5, 50, 500 or 5'000 SKOV3^{GFP}
532 in healthy donor PB. Upon Parsortix enrichment, SKOV3^{GFP} were detected in all spiked samples,
533 including the one carrying five cancer cells where four events were observed (Figure 4C).
534 Subsequently, high depth *TP53* sequencing was performed and the SKOV3 specific c.267delC
535 mutation was detected in all spiked samples (Figure 4D), demonstrating high analytical
536 sensitivity of the approach. No other mutations were identified, suggesting also high analytical
537 specificity, which was furthermore confirmed by analysing four age-matched healthy donors'
538 PBMC (Supplementary Table 1), in which no *TP53* variants were detected
539 (https://www.ncbi.nlm.nih.gov/bioproject/PRJNA1338131). Once analytical validity of deep
540 *TP53* sequencing for both analytes was ensured, plasma cfDNA and Parsortix-enriched
541 corpuscular fraction were sequenced in 15 HGSOC patients (cohort 2, Figure 1B and Figure 1D),
542 to compare CTC and ctDNA-based liquid biopsy performances. In the CTC fraction, 0.58
543 accuracy, 46.7% sensitivity (95% CI: 24.8-69.9%), and 100% specificity (95% CI: 43.9-100%)
544 were achieved (Fisher's exact test p=0.24) (Figure 4E). Specifically, 15 variants in seven patients
545 were detected, with 0.48% median VAF, ranging from 0.21 to 82.9 (Table 2, Figure 4F). On the
546 other hand, cfDNA sequencing, similarly to results obtained in cohort 1, detected 17 variants in
547 12 patients, with median VAF of 1.77% (ranging from 0.34 to 21.73) (Table 2, Figure 4F), and
548 80% disease detection rate, establishing the solid performance of the assay.

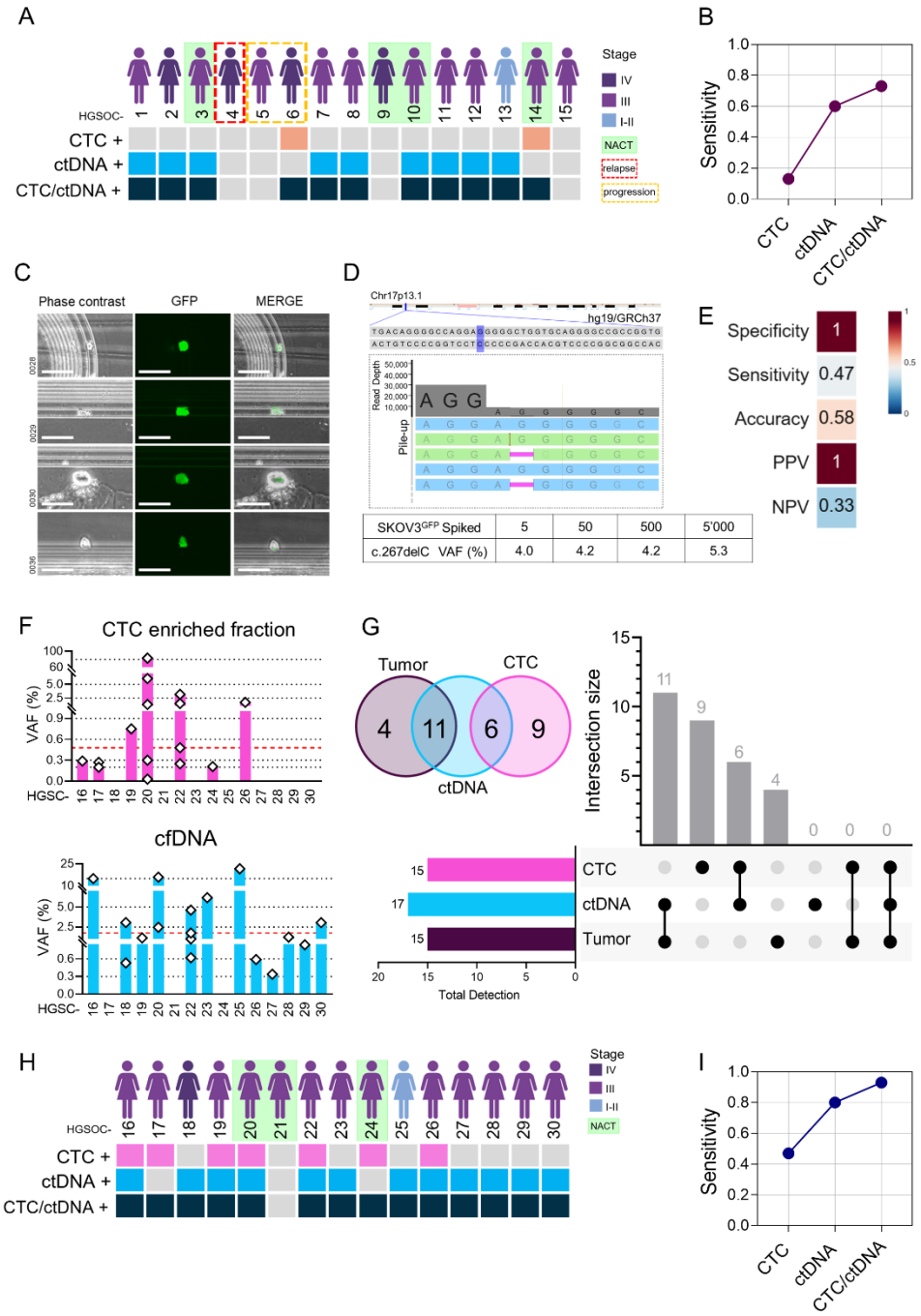

Figure 4. Combining CTC and ctDNA detection in HGSOC liquid biopsies. ***(A)*** *Schematic representation of CTC and ctDNA detection results across cohort 1. Colored and gray squares indicate positive and negative results, respectively. Tumor stage and clinical status are indicated.* ***(B)*** *Sensitivity of CTC, ctDNA, and combined detection assays across cohort 1.* ***(C)*** *Images of four SKOV3^{GFP} captured by Parsortix cassette while processing healthy donor PB spiked with five cells. Scale bar = 100 µm.* ***(D)*** *Representative GenomeBrowser output image of the TP53 NGS of the sample spiked with five SKOV3 cells. The pink bar indicates c.267delC mutation locus, with blue and green bars indicating complementary sequencing reads. Read depth is presented on y-axis. The adjacent table lists TP53 c.267delC VAF found in all spiked samples.* ***(E)*** *Heatmap reporting the performance metrics of tumor-agnostic TP53 sequencing for CTC detection. PPV-positive predictive value; NPV-negative predictive value.* ***(F)*** *TP53 VAFs detected in CTC-enriched fraction (pink) and in plasma cell-free DNA (blue) of cohort 2. Median values are represented by the dashed red lines.* ***(G)*** *Venn diagram and UpSet plot showing shared TP53 variants across tumor tissue, ctDNA and CTC samples. The horizontal bar plot indicates the number of variants found in each analyte, whereas the vertical bar plot shows the number of variants shared between various sample types (Intersection size), according to the black dot intersections found below.* ***(H)*** *Schematic representation of CTC and ctDNA detection results across cohort 2. Colored and gray squares indicate positive and negative results, respectively. Tumor stage and clinical status are indicated.* ***(I)*** *Sensitivity of CTC, ctDNA, and combined detection assays across cohort 2.*

566 To compare genetic heterogeneity between liquid and solid biopsy variants, we retrieved primary
567 tumor TP53 genotyping data which revealed that 35.3% of ctDNA variants were undetected in
568 the solid biopsy (Table 2, Figure 4G). Moreover, variants found in CTC fraction were either
569 private (60%) or shared with ctDNA (40%) (Table 2, Figure 4G). We ruled out the possibility of
570 these being a consequence of clonal haematopoiesis since no TP53 alterations were detected by
571 high-depth sequencing in matching PBMC of patients whose material was available
572 (https://www.ncbi.nlm.nih.gov/bioproject/PRJNA1338131). The latter result, together with the
573 efficient analytical validity assessment, where no unspecific variants were detected in control
574 samples, allowed to reasonably define ctDNA/CTC private variants as true HGSOC-associated
575 events, probably explained by tumor clonal dynamics [53].
576 We next compared the disease detection rate obtained by the two assays in cohort 2 (Figure 4H).
577 One case displayed concordant negativity (6.7%), whereas five patients were positive by both
578 assays (33.3%). Finally, two patients positive for CTCs were concomitantly negative for ctDNA
579 (13.3%) and seven patients positive for ctDNA were negative for CTCs (46.7%), again showing
580 that the combinatory approach increases the ability to detect HGSOC. Specifically, including
581 both analyses in the liquid biopsy protocol increased the sensitivity to 93.3% (Figure 4I).
582 Taken together, ctDNA detection resulted to be more sensitive and more accurate liquid biopsy
583 approach for HGSOC detection compared to CTC-based assays here applied. Provided adequate
584 optimization of CTC identification is achieved, our data imply that tandem CTC/ctDNA analysis
585 may improve clinical utility of liquid biopsy in HGSOC.
586
587
588
589

590 ***Table 2. TP53 variants and their allele frequencies found in liquid and tumor biopsies of cohort 2.*** *fs=frameshift*

HGSOC-	ctDNA VAF (%)	CTC VAF (%)	Tumor VAF (%)	*TP53* variant
16	15.00	0	68.25	p.G112Ffs*33
	0	0.29	0	p.R337C
17	0	0	50.13	p.H179Q
	0	0.27	0	p.D186Efs*61
	0	0.20	0	p.E343Sfs*2
18	3.07	0	36.86	p.I195N
19	1.16	0.75	0	p.R273H
	0.53	0	89.33	p.C275G
20	0	0	32.64	p.L201Cfs*46
	15.98	82.9	0	p.R273H
	2.47	6.07	0	p.K292E
	0	1.30	0	p.V272A
	0	0.29	0	p.Y220C
	0	0.3	0	p.H178P
21	0	0	67.92	p.R175H
22	4.62	3.17	0	p.R273H
	1.77	1.47	0	p.P300A
	0.62	0.48	0	p.K292E
	1.03	0	56.09	p.Y234C
	0	0.25	0	p.L330P
23	6.16	0	87.46	p.R213Hfs*34
24	0	0	70.20	p.L194Sfs*15
	0	0.21	0	p.G226Afs*21
25	21.73	0	75.50	p.C277F
26	0	1.69	0	p.S90Pfs*33
	0.59	0	60.66	p.P153Rfs*24
27	0.34	0	59.00	p.W91*
28	1.25	0	35.64	p.G244C
29	0.84	0	60.05	c.560-1G>A
30	3.06	0	71.38	p.R248W

591

592 **Discussion**

593 Liquid biopsy approaches based on the detection of CTCs or ctDNA have been extensively
594 investigated across a wide range of malignancies for both early cancer detection and prediction
595 of therapeutic response. In certain clinical contexts, these methodologies have already been

596 integrated into routine practice [1], but not in HGSOC, where no screening protocols are
597 currently available, leading most-often to late-stage diagnosis, with consequent high mortality
598 and complicated patient management. Our study represents a step forward in advancing liquid
599 biopsy strategies for HGSOC, demonstrating that while cfDNA analysis outperforms CTC-based
600 assays for disease detection, the combined approach significantly enhances clinical sensitivity
601 compared to either analyte alone. These results highlight the potential translational value of the
602 simultaneous ctDNA and CTCs in HGSOC.
603 It is important to emphasize that, to establish the proof of principle for increased clinical
604 sensitivity of the tandem CTC/ctDNA analysis, a rigorous study design was implemented,
605 ensuring high analytical specificity and sensitivity of each assay prior to clinical validity
606 assessment. In the context of CTC analysis, the three-gene expression assay and *TP53* deep
607 sequencing, both combined with Parsortix enrichment, demonstrated the capability to detect as
608 few as five cancer cells spiked into PB. This level of sensitivity is comparable to that reported
609 for other available methodologies, such as the immunocapture-based AdnaTest Ovarian Cancer
610 Detect [43] and CellSearch [54]. A key strength of our approach was assessing assay specificity
611 by including healthy donor samples as negative controls, which are often omitted in similar
612 studies [43,54], or yield false positive results when included [44]. For ctDNA detection, we
613 employed a laboratory-developed *TP53* sequencing panel coupled to the Ion AmpliSeq HD
614 system. Analytical validity was ensured by empirically identifying 0.31% as the optimal VAF
615 threshold for accurate mutation detection. Given that the reliable calling of low-frequency
616 ctDNA variants (<0.5% VAF) is widely recognized as a critical challenge in the field [33], our
617 established limit of detection represents a meaningful advancement in minimizing false-negative
618 results. Notably, while some studies exclude variants with high allele frequencies to avoid
619 inclusion of germline mutations [55], our data demonstrated that tumor-specific ctDNA variants

620 were frequently present above >1% threshold, highlighting the limitations of such exclusion
621 criteria.
622 Regarding clinical validity, the performance comparison between cfDNA and CTC-based assays
623 revealed the former as a more efficient liquid biopsy strategy. While both showed 100%
624 specificity, cfDNA assay resulted in higher clinical sensitivity, which was either similar (cohort
625 1; 60%) or slightly superior (cohort 2; 80%) to those of previous assays based on *TP53* cfDNA
626 sequencing in HGSOC, reporting clinical sensitivity of 60–73% [22,56,57]. On the other hand,
627 studies evaluating CTCs in OC display a wide range of detection rates, from 15% to 98% [58–
628 63], reflecting substantial methodological heterogeneity. Our findings align with studies
629 reporting lower sensitivity of CTC-based assays, which may be attributed to the stringent
630 specificity criteria defined in our study design. The latter were deliberately selected based on
631 recent evidence indicating that less rigorous methods for capturing OC CTCs are associated with
632 an increased risk of false-positive results [41]. Indeed, during validation of the three-gene
633 expression assay, we observed unexpectedly high expression levels of two keratin-encoding
634 genes in healthy controls, biomarkers frequently used in oncologic liquid biopsy assays [11].
635 This observation underlines the need for caution when incorporating such markers in assays for
636 HGSOC CTC detection. Another explanation for low disease detection rate observed with CTC-
637 based assays could be the technological constraints intrinsic in our approach. We have based our
638 choice of genetic CTC detection with the aim to develop an assay with reasonable turnaround
639 times which could easily be implemented in molecular pathology labs. With hindsight we believe
640 CTC enumeration techniques may provide better performance than here applied genetic methods
641 and should, thus, be considered in future dual-analyte studies.
642 Interestingly, *TP53* sequencing resulted superior compared to the three-gene detection assay for
643 CTC-based HGSOC identification. However, it must be acknowledged that CTC variants were
644 undetected in the matching primary tumor, similarly to more than a third of ctDNA variants

645 found in cohort 2. We excluded this might be due to sequencing errors, since the same high-
646 depth NGS approach revealed no *TP53* variants in healthy donor controls, spiked samples (with
647 exception of the SKOV3 variant) or LGSOC liquid biopsies. Moreover, we excluded the
648 possibility of these being a consequence of clonal hematopoiesis, by sequencing patients'
649 matching PBMCs, allowing to reasonably consider these liquid biopsy private mutations as
650 HGSOC-associated events, possibly explained by clonal dynamics [53], selective
651 immunoclearance of extravasated CTCs [64] or patient cancerous field effect [65]. Such a
652 conclusion is furthermore supported by the fact that all ctDNA variants undetected in primary
653 tissue (35.3%) were shared with those identified in CTCs. In line with our findings, several
654 studies report liquid-biopsy private variants [50–52,66], and clinically relevant tumor genetic
655 heterogeneity has also been observed in HGSOC cfDNA [67,68]. The peculiarity of our finding
656 is that *TP53* mutations are usually considered clonal HGSOC markers [67]. To the best of our
657 knowledge, only a few recent studies, by applying 20,000-30,000 sequencing depth, comparable
658 to here applied NGS approach, find cfDNA private *TP53* variants for which they also exclude
659 clonal hematopoiesis derivation and hypothesize tumor origin [15,69].
660 Importantly, the fact that tumor undetected *TP53* variants where often shared between ctDNA
661 and matched CTC fraction, implies that analyzing both analytes together enables mutation cross-
662 validation, which could permit to avoid invasive tumor biopsy in the first-line blood-based
663 HGSOC screening.
664 Our most relevant finding regards the substantial increase in disease detection rate observed
665 when results of both CTC and ctDNA assays were combined, proving such an approach allows
666 a more efficient liquid biopsy. This is concordant with studies combining CTC and cfDNA
667 analysis in other cancers, which generally agree on the consideration that both analytes broaden
668 the applicability of liquid biopsy in oncologic patients [21,50,66]. Interestingly, Alba-Bernal et
669 al. reveal that, while cfDNA analysis is more efficient in detecting pre-treatment breast tumors,

670 CTCs are found more often than ctDNA in matching post-treatment and post-surgery liquid
671 biopsies, suggesting their particular value when assessing therapy response and minimal residual
672 disease (MDR) [21]. Moreover, similarly to our discovery of private *TP53* variants in CTC
673 fraction, other studies have shown higher genetic heterogeneity of CTCs compared to ctDNA
674 [21], meaning that their investigation could provide complementary data useful for patient
675 management in terms of therapeutic choice. In this context, extending mutation screening to
676 other tumor suppressors and oncogenes associated with HGSOC might discover broader genetic
677 heterogeneity and offer even more informative liquid biopsy.
678 While demonstrating, for the first time, that tandem CTC/ctDNA analysis improves HGSOC
679 liquid biopsy, a limitation remains, which stands in the relatively small cohort of subjects
680 analysed. This prevented us from drawing conclusions on correlation between liquid biopsy
681 results and clinical parameters, such as progression free/overall survival, CA-125 biomarker
682 values or radiology findings. Indeed, the clinical utility of the approach is still to be evaluated,
683 by including a higher proportion of stage I/II cases, as well as longitudinally collected liquid
684 biopsies during the patient follow-up, to allow evaluation of the tandem analysis efficiency for
685 early detection, therapy response prediction and MRD assessment.

686 **Conclusion**

687 Overall, our findings advance liquid biopsy strategies in HGSOC by showing that, while cfDNA
688 outperforms CTCs alone, their combination improves the disease detection rate. Whereas ctDNA
689 provides a sensitive snapshot of tumor burden and enables real-time monitoring of disease
690 dynamics, CTCs reflect historic clonal heterogeneity of the malignancy. The complementary
691 nature of these biomarkers suggests that a multi-analytic approach holds translational potential
692 for integrating liquid biopsy into precision oncology programs of HGSOC, to possibly allow
693 earlier diagnosis, relapse detection, better patient stratification, and anticipate treatment
694 resistance before radiologic progression.

Ethics approval and consent to participate

This study was conducted in accordance with the Declaration of Helsinki and the protocol was approved by the Independent Ethics Committee "Comitato Etico di Area Vasta Emilia Centro" (Protocol EM363-2024_107/2011/U/Tess/AOUBo). All subjects enrolled in the study provided written informed consent for their participation.

Availability of data and materials

All data generated and analysed during this study are included in this published article and its supplementary information file, apart from raw device output data, which are deposited in https://www.ncbi.nlm.nih.gov/bioproject/PRJNA1338131 and https://doi.org/10.6092/unibo/amsacta/8538.

Competing interests

The authors declare that they have no competing interests.

Funding

The research leading to these results has received funding from Italian Ministry of University PRIN 2017, Prot. 2017N7R2CJ to IK and partly from Associazione Italiana Ricerca sul Cancro (AIRC): IG 2020 ID. 24494 project to A.Ma.P. and IG 2019–ID. 22921 project to G.Ga.

Authors' contributions

Conceptualization, B.C., I.K.; methodology, B.C., D.d.B.; acquisition and analysis, B.C., S.Cor., M.D.L., S.L., C.A.C., G. Gi., S. Col., A.D.L., D.d.B., I.K.; data interpretation: B.C., S.d.C., F.M., P.D.I., A.Ma.P., A.My.P., D.d.B., G.Ga., I.K.; writing – original draft, B.C., I.K., writing – review & editing, B.C., C.A.C, A.Ma.P., A.My.P., D.d.B., G.Ga, I.K.; project administration, I.K., funding acquisition and resources, A.Ma.P., G.Ga., I.K. All authors have approved the submitted version of the work and have agreed both to be personally accountable for the author's own contributions and to ensure that questions related to the accuracy or integrity of any part of the work, even ones in which the author was not personally involved, are appropriately investigated, resolved, and the resolution documented in the literature.

References

[1] Ignatiadis M, Sledge GW, Jeffrey SS. Liquid biopsy enters the clinic — implementation issues and future challenges. Nat Rev Clin Oncol 2021;18:297–312. https://doi.org/10.1038/s41571-020-00457-x.

[2] Cancer of the Ovary - Cancer Stat Facts (2025). SEER n.d. https://seer.cancer.gov/statfacts/html/ovary.html.

[3] De Leo A, Santini D, Ceccarelli C, Santandrea G, Palicelli A, Acquaviva G, et al. What Is New on Ovarian Carcinoma: Integrated Morphologic and Molecular Analysis Following the New 2020 World Health Organization Classification of Female Genital Tumors. Diagn Basel Switz 2021;11:697. https://doi.org/10.3390/diagnostics11040697.

[4] Huang C, Lin X, He J, Liu N. Enrichment and detection method for the prognostic value of circulating tumor cells in ovarian cancer: A meta-analysis. Gynecol Oncol 2021;161:613–20. https://doi.org/10.1016/j.ygyno.2021.02.024.

[5] He X, Li S, Ni Y, Jin M, Fu X. A meta-analysis of the prognostic value of circulating tumor cells in ovarian cancer. Am J Transl Res 2022;14:3574–83.

742 [6] Lemma S, Perrone AM, De Iaco P, Gasparre G, Kurelac I. Current methodologies to
743 detect circulating tumor cells: a focus on ovarian cancer. Am J Cancer Res 2021;11:4111–26.
744 [7] CellSearch - Circulating Tumor Cell test Menarini n.d. https://www.cellsearchctc.com/.
745 [8] Lin D, Shen L, Luo M, Zhang K, Li J, Yang Q, et al. Circulating tumor cells: biology and
746 clinical significance. Signal Transduct Target Ther 2021;6:404. https://doi.org/10.1038/s41392-
747 021-00817-8.
748 [9] Obermayr E, Maritschnegg E, Agreiter C, Pecha N, Speiser P, Helmy-Bader S, et al.
749 Efficient leukocyte depletion by a novel microfluidic platform enables the molecular detection
750 and characterization of circulating tumor cells. Oncotarget 2018;9:812–23.
751 https://doi.org/10.18632/oncotarget.22549.
752 [10] Kolostova K, Pinkas M, Jakabova A, Pospisilova E, Svobodova P, Spicka J, et al.
753 Molecular characterization of circulating tumor cells in ovarian cancer. Am J Cancer Res
754 2016;6:973–80.
755 [11] Rushton AJ, Nteliopoulos G, Shaw JA, Coombes RC. A Review of Circulating Tumour
756 Cell Enrichment Technologies. Cancers 2021;13:970. https://doi.org/10.3390/cancers13050970.
757 [12] Giannopoulou L, Mastoraki S, Buderath P, Strati A, Pavlakis K, Kasimir-Bauer S, et al.
758 ESR1 methylation in primary tumors and paired circulating tumor DNA of patients with high-
759 grade serous ovarian cancer. Gynecol Oncol 2018;150:355–60.
760 https://doi.org/10.1016/j.ygyno.2018.05.026.
761 [13] Parkinson CA, Gale D, Piskorz AM, Biggs H, Hodgkin C, Addley H, et al. Exploratory
762 Analysis of TP53 Mutations in Circulating Tumour DNA as Biomarkers of Treatment Response
763 for Patients with Relapsed High-Grade Serous Ovarian Carcinoma: A Retrospective Study. PLoS
764 Med 2016;13:e1002198. https://doi.org/10.1371/journal.pmed.1002198.
765 [14] Calapre L, Giardina T, Beasley AB, Reid AL, Stewart C, Amanuel B, et al. Identification
766 of TP53 mutations in circulating tumour DNA in high grade serous ovarian carcinoma using next

767 generation sequencing technologies. Sci Rep 2023;13:278. https://doi.org/10.1038/s41598-023-
768 27445-2.
769 [15] Heo J, Kim Y-N, Shin S, Lee K, Lee J-H, Lee YJ, et al. Serial Circulating Tumor DNA
770 Analysis with a Tumor-Naïve Next-Generation Sequencing Panel Detects Minimal Residual
771 Disease and Predicts Outcome in Ovarian Cancer. Cancer Res 2024;84:468–78.
772 https://doi.org/10.1158/0008-5472.CAN-23-1429.
773 [16] Ahmed AA, Etemadmoghadam D, Temple J, Lynch AG, Riad M, Sharma R, et al. Driver
774 mutations in TP53 are ubiquitous in high grade serous carcinoma of the ovary. J Pathol
775 2010;221:49–56. https://doi.org/10.1002/path.2696.
776 [17] Cancer Genome Atlas Research Network. Integrated genomic analyses of ovarian
777 carcinoma. Nature 2011;474:609–15. https://doi.org/10.1038/nature10166.
778 [18] Wishart G, Templeman A, Hendry F, Miller K, Pailhes-Jimenez A-S. Molecular Profiling
779 of Circulating Tumour Cells and Circulating Tumour DNA: Complementary Insights from a
780 Single Blood Sample Utilising the Parsortix® System. Curr Issues Mol Biol 2024;46:773–87.
781 https://doi.org/10.3390/cimb46010050.
782 [19] Haber DA, Velculescu VE. Blood-Based Analyses of Cancer: Circulating Tumor Cells
783 and Circulating Tumor DNA. Cancer Discov 2014;4:650–61. https://doi.org/10.1158/2159-
784 8290.CD-13-1014.
785 [20] ©2025 - ClinCalc LLC. n.d. https://clincalc.com/stats/Power.aspx.
786 [51] Shaw JA, Guttery DS, Hills A, Fernandez-Garcia D, Page K, Rosales BM, et al. Mutation
787 Analysis of Cell-Free DNA and Single Circulating Tumor Cells in Metastatic Breast Cancer
788 Patients with High Circulating Tumor Cell Counts. Clin Cancer Res Off J Am Assoc Cancer Res
789 2017;23:88–96. https://doi.org/10.1158/1078-0432.CCR-16-0825.
790 [52] Kong SL, Liu X, Tan SJ, Tai JA, Phua LY, Poh HM, et al. Complementary Sequential
791 Circulating Tumor Cell (CTC) and Cell-Free Tumor DNA (ctDNA) Profiling Reveals Metastatic

792 Heterogeneity and Genomic Changes in Lung Cancer and Breast Cancer. Front Oncol
793 2021;11:698551. https://doi.org/10.3389/fonc.2021.698551.
794 [53] Gremmelspacher D, Gawron J, Szczerba BM, Jahn K, Castro-Giner F, Kuipers J, et al.
795 Phylogenetic inference reveals clonal heterogeneity in circulating tumor cell clusters. Nat Genet
796 2025;57:1357–61. https://doi.org/10.1038/s41588-025-02205-2.
797 [54] Banys-Paluchowski M, Fehm T, Neubauer H, Paluchowski P, Krawczyk N, Meier-
798 Stiegen F, et al. Clinical relevance of circulating tumor cells in ovarian, fallopian tube and
799 peritoneal cancer. Arch Gynecol Obstet 2020;301:1027–35. https://doi.org/10.1007/s00404-020-
800 05477-7.
801 [55] Barbosa A, Pinto P, Peixoto A, Guerra J, Pinheiro M, Santos C, et al. Next Generation
802 Sequencing of Tumor and Matched Plasma Samples: Identification of Somatic Variants in
803 ctDNA From Ovarian Cancer Patients. Front Oncol 2021;11:754094.
804 https://doi.org/10.3389/fonc.2021.754094.
805 [56] Heitz F, Lakis S, Harter P, Heikaus S, Sehouli J, Talwar J, et al. Cell-free tumor DNA,
806 CA125 and HE4 for the objective assessment of tumor burden in patients with advanced high-
807 grade serous ovarian cancer. PLOS ONE 2022;17:e0262770.
808 https://doi.org/10.1371/journal.pone.0262770.
809 [57] Shen W, Shan B, Liang S, Zhang J, Yu Y, Zhang Y, et al. Hybrid Capture-based Genomic
810 Profiling of Circulating Tumor DNA From Patients With Advanced Ovarian Cancer. Pathol
811 Oncol Res POR 2021;27:581534. https://doi.org/10.3389/pore.2021.581534.
812 [58] Salmon C, Levermann J, Neves RPL, Liffers S-T, Kuhlmann JD, Buderath P, et al. Image-
813 Based Identification and Genomic Analysis of Single Circulating Tumor Cells in High Grade
814 Serous Ovarian Cancer Patients. Cancers 2021;13:3748.
815 https://doi.org/10.3390/cancers13153748.

816 [59] Kim M, Suh DH, Choi JY, Bu J, Kang Y-T, Kim K, et al. Post-debulking circulating
817 tumor cell as a poor prognostic marker in advanced stage ovarian cancer: A prospective
818 observational study. Medicine (Baltimore) 2019;98:e15354.
819 https://doi.org/10.1097/MD.0000000000015354.
820 [60] Dent BM, Ogle LF, O'Donnell RL, Hayes N, Malik U, Curtin NJ, et al. High-resolution
821 imaging for the detection and characterisation of circulating tumour cells from patients with
822 oesophageal, hepatocellular, thyroid and ovarian cancers. Int J Cancer 2016;138:206–16.
823 https://doi.org/10.1002/ijc.29680.
824 [61] Chebouti I, Kasimir-Bauer S, Buderath P, Wimberger P, Hauch S, Kimmig R, et al. EMT-
825 like circulating tumor cells in ovarian cancer patients are enriched by platinum-based
826 chemotherapy. Oncotarget 2017;8:48820–31. https://doi.org/10.18632/oncotarget.16179.
827 [62] Lee M, Kim EJ, Cho Y, Kim S, Chung HH, Park NH, et al. Predictive value of circulating
828 tumor cells (CTCs) captured by microfluidic device in patients with epithelial ovarian cancer.
829 Gynecol Oncol 2017;145:361–5. https://doi.org/10.1016/j.ygyno.2017.02.042.
830 [63] Kim NK, Suh DH, Kim K, No JH, Kim YB, Kim M, et al. High-throughput viable
831 circulating tumor cell isolation using tapered-slit membrane filter-based chipsets in the
832 differential diagnosis of ovarian tumors. PloS One 2024;19:e0304704.
833 https://doi.org/10.1371/journal.pone.0304704.
834 [64] Strilic B, Offermanns S. Intravascular Survival and Extravasation of Tumor Cells. Cancer
835 Cell 2017;32:282–93. https://doi.org/10.1016/j.ccell.2017.07.001.
836 [65] Chai H, Brown RE. Field effect in cancer-an update. Ann Clin Lab Sci 2009;39:331–7.
837 [66] Markou AN, Londra D, Stergiopoulou D, Vamvakaris I, Potaris K, Pateras IS, et al.
838 Preoperative Mutational Analysis of Circulating Tumor Cells (CTCs) and Plasma-cfDNA
839 Provides Complementary Information for Early Prediction of Relapse: A Pilot Study in Early-

840 Stage Non-Small Cell Lung Cancer. Cancers 2023;15:1877.
841 https://doi.org/10.3390/cancers15061877.
842 [67] Paracchini L, Mannarino L, Beltrame L, Landoni F, Fruscio R, Grassi T, et al. Targeted
843 Mutational Analysis of Circulating Tumor DNA to Decipher Temporal Heterogeneity of High-
844 Grade Serous Ovarian Cancer. Cancers 2022;14:3697. https://doi.org/10.3390/cancers14153697.
845 [68] Gerratana L, Movarek M, Wehbe F, Katam N, Mahalingam D, Donahue J, et al. Genomic
846 Landscape of Advanced Solid Tumors in Circulating Tumor DNA and Correlation With Tissue
847 Sequencing: A Single Institution's Experience. JCO Precis Oncol 2022:e2100289.
848 https://doi.org/10.1200/PO.21.00289.
849 [69] Lheureux S, Prokopec SD, Oldfield LE, Gonzalez-Ochoa E, Bruce JP, Wong D, et al.
850 Identifying Mechanisms of Resistance by Circulating Tumor DNA in EVOLVE, a Phase II Trial
851 of Cediranib Plus Olaparib for Ovarian Cancer at Time of PARP Inhibitor Progression. Clin
852 Cancer Res Off J Am Assoc Cancer Res 2023;29:3706–16. https://doi.org/10.1158/1078-
853 0432.CCR-23-0797.
854